Zakhireh et al., *BioImpacts*, 2022, 12(3), 183-193
doi: 10.34172/bi.2021.24
http://bi.tbzmed.ac.ir/

Hollow pollen grains as scaffolding building blocks in bone tissue engineering

Solmaz Zakhireh[1,2], Jaleh Barar[3,4*], Younes Beygi-Khosrowshahi[5], Abolfazl Barzegari[3], Yadollah Omidi[6], Khosro Adibkia[1,3,4*]

[1]Drug Applied Research Center, Tabriz University of Medical Sciences, Tabriz, Iran
[2]Student Research Committee, Tabriz University of Medical Sciences, Tabriz, Iran
[3]Research Center for Pharmaceutical Nanotechnology, Biomedicine Institute, Tabriz University of Medical Sciences, Tabriz, Iran
[4]Department of Pharmaceutics, Faculty of Pharmacy, Tabriz University of Medical Sciences, Tabriz, Iran
[5]Chemical Engineering Department, Faculty of Engineering, Azarbaijan Shahid Madani University, Tabriz, Iran
[6]Department of Pharmaceutical Sciences, College of Pharmacy, Nova Southeastern University, Fort Lauderdale, FL 33328, USA

Article Info

Article Type:
Original Article

Article History:
Received: 16 July 2020
Revised: 17 Oct. 2020
Accepted: 18 Oct. 2020
ePublished: 18 Dec. 2021

Keywords:
Pollen grain,
Pistacia vera L.,
Bottom-up tissue engineering,
Building block,
Bone tissue,
Human adipose-derived mesenchymal stem cells

Abstract

Introduction: The current study, for the first time, suggests nature-made pollen grains (PGs) of *Pistacia vera* L. as a potential candidate for using as scaffolding building blocks with encapsulation capability of bioactive compounds, such as bone morphogenetic protein 4 (BMP4).

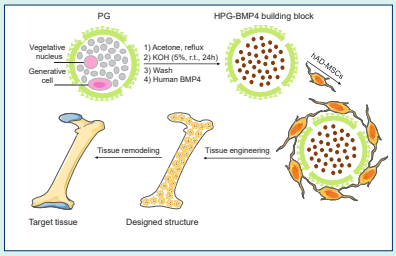

Methods: A modified method using KOH (5%, 25°C) was developed to produce nonallergic hollow pollen grains (HPGs), confirmed by energy dispersive X-ray (EDX) analysis, field emission scanning electron microscopy (FESEM), and DNA and protein staining techniques. The *in-vitro* study was conducted on human adipose-derived mesenchymal stem cells (hAD-MSCs) to investigate the applicability of HPGs as bone scaffolding building blocks. Cytocompability was evaluated by FESEM, MTT assay, and gene expression analysis of apoptotic markers (BAX and BCL2). The osteoconductive potential of HPGs was assessed by alkaline phosphatase (ALP) activity measurement and gene expression analysis of osteogenic markers (RUNX2 and osteocalcin).

Results: Findings demonstrated that HPGs can be considered as biocompatible compounds increasing the metabolic activities of the cells. Further, the bioactive nature of HPGs resulted in suitable cellular adhesion properties, required for a potent scaffold. The investigation of apoptotic gene expression indicated a reduced BAX/BCL2 ratio reflecting the protective effect of HPGs on hAD-MSCs. The increased ALP activity and expression of osteogenic genes displayed the osteoconductive property of HPGs. Moreover, the incorporation of BMP4 in HPGs initiated a synergistic effect on osteoblast maturation.

Conclusion: Owing to the unique compositional and surface nanotopographical features of the *Pistacia vera* L. HPG, this microscale architecture provides a favorable microenvironment for the bottom-up remodeling of bone.

Introduction

Regeneration of the unrepairable bone defects as the main causes of functional disabilities and esthetic deformities remains an important concern in medicine. In recent years, tissue engineering and regenerative medicine (TERM) using the key elements (scaffold, cells, and signaling molecules) provides an efficient opportunity for advancing this field. Undoubtedly, the major challenge in TERM is to design effective scaffolds, with intrinsic stimulatory/modulatory impact on the cells toward the generation of the desired tissue. Further, novel scaffold systems, with the capability of encapsulation and on-demand release of multiple growth factors have recently been developed to induce desirable cell functions for promoting bone regeneration.[1,2] The on-site release of growth factors from biomaterial scaffolds has been shown to accelerate bone formation.[3] However, vascularization and mass transfer limitations are great impediments in the

*Corresponding authors: Khosro Adibkia, Email: adibkia@tbzmed.ac.ir; Jaleh Barar, Email: jbarar@tbzmed.ac.ir

engineering of the living tissue constructs. It has also been reported that a superficial thin tissue layer is supported with an adequate mass transfer, while the cells at deeper layers may face nutritional deprivation resulting in a cellular phase transformation. Currently, an engineering strategy namely the "bottom-up" approach has emerged. In this biomimetic approach, the microstructure modular tissues, as the building blocks, is initially prepared using the stem cells and subsequently assembles to produce complex macrostructure close-to-native tissue. This modular approach can offer several advantages such as homogeneous cell distribution, designing 3D microenvironments to modulate stem cell phenotype, preventing agglomeration, providing necessary components during cell expansion without thickness limitation, providing a high-cell density, and generating 3D constructs with no size limitation.[4,5] Two main approaches are utilized for the fabrication of tissue from microscale building blocks, which include (i) a suspension of cells and scaffolding building blocks or cell-cultured building blocks are injected into a damaged site, and (ii) the cell-cultured building blocks are assembled within a bioreactor to produce native tissue-like implants.[6,7]

Nature offers the excellently engineered microstructure of pollen grains (PGs) as the scaffolding building blocks with interior core and exterior shell usability. PG is a male sex cell produced by seed plants and comes in a wide variety of shapes and sizes ranging from 5 to 250 μm. It contains vegetative and generative cells surrounded by a sophisticated wall made of two main layers, inner intine, and very inert and tough outer exine. Intine is close to the plasma membrane and predominantly made of cellulose. Exine is essentially made of one of the most advanced polymers in nature known as sporopollenin, a highly cross-linked copolymer composed of an aliphatic backbone of the long-chain fatty acids and aromatic side chains cross-linked by the ester or ether bonds.[8,9] Carboxyl and hydroxyl functional groups along with the aliphatics give amphiphilic nature to the sporopollenin. Wall porosity with pore sizes of up to 40 nm and channels with an approximate diameter of 200–300 nm make the pollen extremely permeable.[10,11] These characteristics allow the extraction of materials constituted the inner cavity, which results in the production of the hollow pollen grain (HPG) for encapsulation of the bioactive compounds in a wide variety of sizes and polarities. The residual shell has the advantages of being nonallergic and nontoxic.[12] Besides the structural features, pollens exhibit outstanding properties, including biocompatibility, biodegradability, renewability, low density and high surface area as well as desirable desirable mechanical properties. Furthermore, pollens exhibit some medicinal effects including antibacterial, antiviral, antifungal, antioxidant, anticancer, anti-inflammatory, antiradiation, hepatoprotective, immune-enhancing, local analgesic, red blood cells-enhancing growth-enhancing, anti-aging, and bone formation stimulatory impacts. Biological activities of the pollen are associated with phenolic compounds, mostly flavonoids that are accumulated in sporopollenin and have a great modulatory effect on pollen development and germination.[13-16]

Cellular behavior, ranging from initial adhesion to later differentiation, is strongly influenced by the scaffold surface characteristics such as topography (i.e., roughness and porosity) and the chemical composition. Surface engineering using advanced technologies endeavors to design the scaffolds with functionalized nanotopographically patterned surfaces to provide a bioactive surface for promoting the alignment of cells and extracellular matrix (ECM), cell-scaffold integration, and directed cell responses.[17-19] Therefore, it is hypothesized that the micro-sized pollen of *Pistacia vera* L. with bead-like shape structure and intrinsic nanotopographical and chemical factors can be a suitable candidate for application as a natural bioactive building block with an encapsulation capability of the bioactive compounds.

The use of stem cells has greatly facilitated the tissue formation process and has revolutionized the TERM due to displaying exceptional properties such as self-regeneration and a high potential for differentiation into the target tissue with no stimulation of the immune response. Human adipose-derived mesenchymal stem cells (hAD-MSCs) are an ideal cell source for the TERM applications, in large part due to their multipotency, abundance, and accessibility.[20,21]

In the current study, a modified simple and mild method was developed for obtaining the intact nonallergic HPGs of *P. vera*, which then was further explored *in-vitro* through cytotoxicity, biocompatibility, and also osteoconductive property for application as modular scaffolds, using hAD-MSCs. Cytocompability was investigated by field emission scanning electron microscopy (FESEM), MTT assay, and the expression of apoptotic genes (BAX and BCL2) analyses. Alkaline phosphatase (ALP) activity was measured to evaluate the possible osteoconductive potential of the HPGs. Ultimately, an osteogenic differentiation signaling molecule of the bone morphogenetic protein 4 (BMP4) was encapsulated into the HPGs (HPGs-BMP4) to examine the encapsulation capability of the developed building blocks in directed cell differentiation. Afterward, expression of the osteogenic genes (RUNX2 and osteocalcin) was assessed to monitor the osteogenesis of hAD-MSCs grown on the HPGs and HPGs-BMP4 building blocks.

Materials and Methods

Materials

The mature PGs of Pistachio (*Pistacia vera* L.) were collected from male flowers in early spring in Qazi Jahan Pistachio gardens, Iran. The hAD-MSCs were obtained from the Iranian Biological Resource Center (Tehran, Iran). Trypan blue solution (0.4%) and 3-(4,5-Dimethyl-

2-thiazolyl)-2,5-diphenyl-2H-tetrazolium bromide (MTT) were purchased from Sigma-Aldrich (Poole, UK). TRIzol reagent and reverse transcriptase reagent kit were bought from Thermo Fisher Scientific (Waltham, MA, USA). Maxima SYBER Green qPCR master mix was obtained from BioFACT (Daejeon, Korea). Cell culture flasks, well plates, and pipettes were purchased from SPL Life Sciences (Pocheon, South Korea). All cell culture media and components were provided from Gibco, Life Technologies (Paisley, UK). The oligonucleotide primer sequences were received from Takapo Zist Company (Tehran, Iran). Other chemicals were supplied from Merck (Kenilworth, NJ, USA).

Preparation of HPGs

PGs (10 g) were first defatted by stirring in acetone under reflux condition for 4 hours, with the refreshing of the solvent after 2 hours. Particles were filtered, rinsed with acetone, and dried overnight in the open air. After defatting, several chemical methods were examined to remove sporoplasmic materials (e.g., nucleic acids, proteins, carbohydrates, and lipids)[22,23], as follows:

(i) The defatted PGs were suspended in KOH(aq) solution (5% w/v, 30 mL) and stirred under reflux at 80˚C for 12 hours. The suspension was filtered, rinsed thrice with hot water and twice with hot ethanol, and dried.

(ii) The defatted PGs (2 g) were suspended in H_3PO_4 (85% v/v, 15 mL) and refluxed at 70˚C for 10 hours under gentle stirring. The suspension was filtered and since nothing was collected, no rinsing was done.

(iii) The defatted PGs (3 g) were suspended in KOH(aq) solution (5% w/v, 15 mL) and stirred gently at room temperature for 24 or 48 hours, the suspension was then well rinsed with hot water and ethanol, vacuum-filtered, and dried.

Field emission scanning electron microscopy with energy dispersive X-ray analysis (FESEM-EDX)

The surface characteristics (e.g., size, shape, pores, and exine pattern) of raw PGs and the processed PGs were evaluated by field emission scanning electron microscopy (FESEM; MIRA3, Tescan Company, Brno, Czech). Samples were affixed to the aluminum stubs with double-sided adhesive tapes and coated with gold to obtain a layer of 150 Å thicknesses using a sputter coater (Emitech K550, Kent, UK). Images were captured at different magnifications by means of an operating voltage of 10 kV.

To evaluate the protein content, the nitrogen measurement of the above-mentioned samples was performed by way of EDX analysis.

DNA and protein content staining

The samples (raw and processed PGs) were fixed in 50% ethanol-formalin-acetic acid (90:5:5, v/v/v) for about 24 hours, dehydrated in a graded ethanol series, cleared in xylene, and embedded in paraffin. Sections of 10 µm thickness were prepared by using a rotary microtome (R. Jung, Heidelberg, Germany). Then, the slides were deparaffinized in xylene, rehydrated in a graded ethanol series, and stained. Detection of DNA was done according to the Feulgen technique,[24] a DNA-specific staining technique. The protein recognition was performed by the Comasi Brilliant Blue method,[25] as the most frequently used protein staining dye. Finally, the samples were investigated by an optical microscope (N800-F, Jiangsu, China) and photographed by a microscope camera (TrueChrome Metrics, Tucsen, China).

Encapsulation of BMP4 into HPGs

HPGs (2 mg) were suspended in the aqueous solution of 100 ng human BMP4 and freeze-dried under vacuum using a freeze dryer (Telstar LyoQuest, Spain) to obtain BMP4-encapsulated HPGs (HPGs-BMP4).

Cell culture

Primary hAD-MSCs were used to investigate the influence of HPGs as scaffolding building blocks on the behavior of the cell. HPGs (2 mg) were placed in each well of a 24-well plate and sterilized using 70% (v/v) ethanol solution for 1 h, then dried and washed twice in PBS for 30 minutes. The cells were seeded at a density of 3500 cells per well and incubated with the basal medium of DMEM/F12 containing l-glutamine/10% FBS/1% antibiotics at 37˚C in a humidified atmosphere of 5% CO_2 incubator (ASTEC, Fukuoka, Japan). The medium was replaced every 48 hours.

To investigate the synergistic differentiation behavior, two test groups of HPGs and HPGs-BMP4 were used. Osteogenic differentiation culture medium was constituted of the basal medium supplemented with dexamethasone (10 nM), β-glycerophosphate (10 mM), and ascorbic acid (50 µM).

FESEM analysis of cell-seeded HPGs building blocks

To visualize cultured hAD-MSCs behaviors (e.g., morphology, attachment, and spreading in the presence of HPGs building blocks), the field emission scanning electron microscopy (FESEM; MIRA3, Tescan Company, Brno, Czech) was employed. For this purpose, after 1 day of culture, cell-seeded HPGs were gently washed with PBS, fixed in 4% (w/v) formaldehyde/PBS for 20 minutes at 4˚C, and rinsed with deionized water. Finally, behavior of the cell was monitored and photographed at the interface with building blocks.

Cytocompatibility evaluation

The metabolic activities of cells were studied to evaluate the cytocompatibility of the HPGs building blocks. The cells were cultured on the HPGs and then were subjected to MTT [3-(4,5-dimethylthiazol-2-yl)-2,5-diphenyltetrazolium bromide] assay after 7, 14, and 21 days. To this end, after the incubation period, 50 µL of

MTT solution (5 mg/mL in DMEM/F12) was added per well at a final volume of 500 µL. After 3 hours incubation, the medium was removed and the purple formazan crystals, produced by viable cells with metabolic activity, were dissolved by adding 200 µL of isopropanol to each well. The dye-containing solution was then transferred to a 96-well plate. Cell metabolic activity was measured as optical density (OD) values using a microplate reader (Elx808, BioTek, USA) at an excitation wavelength of 570 nm.

ALP activity measurement

The osteoconductive potential of *P. vera* HPGs building blocks was assessed by measuring ALP activity. On days 7, 14, and 21 of the culture, the cells cultured on HPGs were washed with PBS (×3), lysed with lysis buffer containing buffer stock solution (composed of 1.5 M Tris–HCl, 1 mM $ZnCl_2$, and 1mM $MgCl_2{\cdot}6H_2O$) diluted 10X in dH_2O and 1% of Triton X-100, incubated at 37˚C for 30 minutes, and kept at 4˚C overnight. Subsequently, cell lysates were collected, vortexed, and centrifuged. To evaluate ALP activity, the mixture of 190 µL of ALP substrate solution (37.1 mg of p-nitrophenyl phosphate (pNPP) in 20 mL of buffer stock solution) and 10 µL of the cell lysate was prepared in a 96-well plate, incubated in the dark for 50 minutes at room temperature. Finally, the absorbance was determined by the fluorescence microscope system at 405 nm (Cytation 5, BioTek, USA).

Gene expression analysis

RNA extraction and cDNA synthesis

Total RNA was extracted from the cells on days 7, 14, and 21 using TRIzol reagent according to the manufacturer recommendations. To obtain pure RNA, additional steps including chloroform-induced phase separation, ethanol precipitation, and washing were involved. The RNA pellet was dissolved in 50 µL of diethylpyrocarbonate (DEPC) water and kept at -70˚C. The quality and quantity of RNAs were determined by measuring the ratio of DNA optical density to protein optical density (A260/A280 Ratio) with NanoDrop 1000 Spectrophotometer (NanoDrop, Wilmington, USA). The first stranded cDNA was synthesized in a total volume of 20 µL reverse transcription (RT) reaction mixture using the cDNA Synthesis Kit in two steps. In the first step, a mixture of 1 µL random hexamer (2.5 ng/µL), DEPC water, and extracted RNA was prepared in a total volume of 12 µL and incubated at 65˚C for 5 minutes. In the second step, a mixture of 4 µL 5X RT Buffer, 1 µL M-MuLV reverse transcriptase (100U/µL), 1 µL RNase inhibitor (20U/µL), 1 µL dNTP mix, and 1 µL DEPC water was prepared and added to the first step mixture.

Reverse transcription was performed using SimpliAmp Thermal Cycler (Applied Biosystems, Thermo Fisher Scientific, Waltham, MA, USA) as follows: 25˚C (10 minutes) followed by incubation at 42˚C (60 minutes) and 75˚C (10 minutes).

Quantitative polymerase chain reaction (qPCR)

The expressions of BCL2-associated X protein (*BAX*), B-cell lymphoma 2 (*BCL2*), Runt-related transcription factor 2 (*RUNX2*), and osteocalcin (*OSC*) genes were analyzed by Bio-Rad iQ5 amplification system (Bio-Rad Laboratories Inc., Hercules, USA). Table 1 shows primer sequences designed for gene expression detection. Reaction mixture included: 1 µL diluted cDNA, 10 µL 2X Power SYBR Green PCR Master Mix, 0.5 µL of each forward and reverse primer (200 nM), and 8 µL DEPC water. Owing to the stability of Glyceraldehyde 3-phosphate dehydrogenase (GAPDH) during the osteogenesis of MSCs after 14 and 20 days, it was used as a housekeeping gene to normalize target gene expression in qRT-PCR assays.[26]

The cycle steps were programmed as below: an initial denaturation step of 94˚C (5 minutes), followed by 35 cycles of 94˚C (30 seconds), annealing step as mentioned temperature in Table 1 (30 seconds), extension step of 72˚C (30 seconds), and final amplification step of 72˚C (10 minutes).

The relative expression of target genes was calculated using Michael W. Pfaffl's method[27]:

Table 1. Primer sequences used for qPCR analysis

Gene	Primer sequence	Annealing Temperature (˚C)
BAX	Forward: 5′-GATGCGTCCACCAAGAAG-3′ Reverse: 5′-AGTTGAAGTTGCCGTCAG-3′	52
BCL2	Forward: 5′-GTTCCCTTTCCTTCCATCC-3′ Reverse: 5′-TAGCCAGTCCAGAGGTGAG-3′	57
RUNX2	Forward: 5′-CAGACCAGCAGCACTCCATA-3′ Reverse: 5′-CAGCGTCAACACCATCATTC-3′	59
OSC	Forward: 5′-CAGCGAGGTAGTGAAGAGAC-3′ Reverse: 5′-GCCAACTCGTCACAGTCC-3′	56.5
GAPDH	Forward: 5′-CCTGCTTCACCACCTTCTTG-3′ Reverse: 5′-CCATCACCATCTTCCAGGAG-3′	58.5

$Ratio = (E_{target})^{\Delta CP}{}_{target\ (control-sample)} / (E_{ref})^{\Delta CP}{}_{ref\ (control-sample)}$

E: real-time PCR efficiencies, ΔCP: crossing point difference

Statistical analysis

All data resulted from cell viability, ALP activity, and qRT-PCR analyses were displayed as mean ± standard deviation (SD) carried out in triplicate. Statistical analyses were performed using the Mann-Whitney U test with a *P* value of less than 0.05 regarded as statistical significance.

Results

Particle size, surface morphology, and core materials removal

The particle size and surface morphology play an important role in the performance of PGs as scaffolding building blocks. The images of surface morphology obtained by FESEM revealed that PGs of *P. vera* possess a unique microstructure with spherical geometries in uniform size of about 27 µm. Observed wrinkles were due to the flexibility and elasticity of the pollen wall.[28] The exine showed a dense reticulate-homobrochate sculpture pattern with several germinal apertures (Fig. 1A). As shown in Fig. 1B, the alkaline lysis process using 5% (w/v) KOH(aq) at 80˚C caused severe damages to the pollen microstructure and the loss of the surface decoration. The other common method used to evacuate the grains, i.e. acidolysis process using phosphoric acid (85% v/v) at 70˚C, resulted in complete decomposition of PGs. Therefore, to avoid damage and decomposition of the PGs, alkaline treatment in mild conditions was undertaken. The FESEM images showed that alkaline lysis at room temperature for 48 hours led to the loss of integrity and rupture of the PGs; nevertheless, the surface decorations were maintained. The cross-sectional image of the un-washed HPGs showed the entrapment of exudate starch granules and protein bodies[29] in the ruptured pollen cavities (Fig. 1C). Reduced exposure time from 48 to 24 hours to the alkali condition resulted in the successful removal of the core material from the germinal apparatus while maintaining the integrity, nanostructure, and surface decoration of PGs (Fig. 1D). Further, the impact of extensive washing step on HPGs was evaluated and illustrated in Fig. 1E.

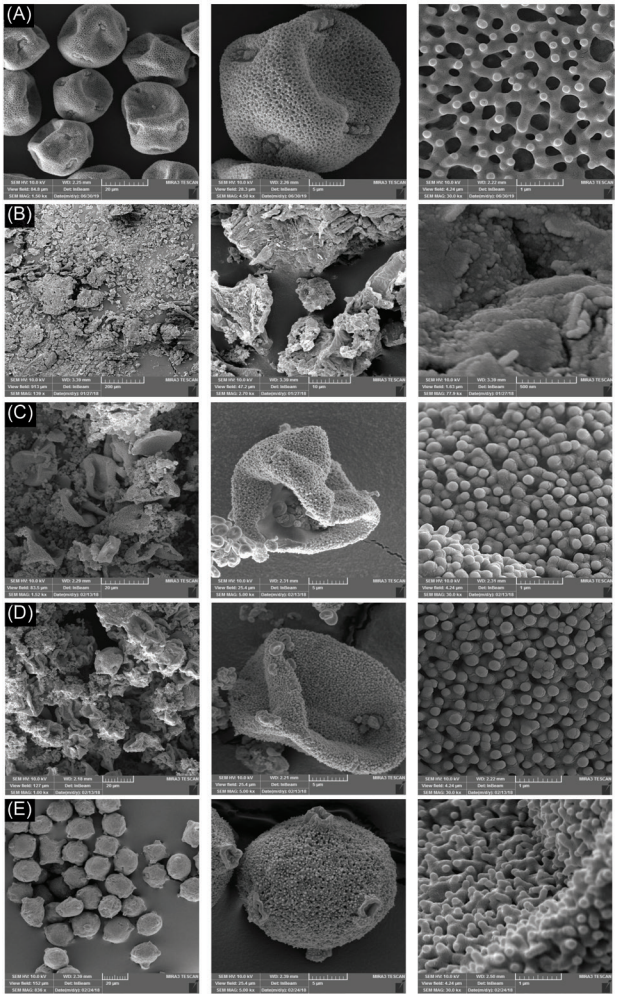

Fig. 1. FESEM images of the *Pistacia vera* L. PGs at various empty process conditions. (A) Raw PGs. PGs treated with (B) KOH (5% w/v, 12 h reflux), (C) KOH (5% w/v, 48h) before washing step, (D) KOH (5% w/v, 24 h) before washing step, and (E) KOH (5% w/v, 24h) after washing step. The micrographs show different magnifications. PG: pollen grain. HPG: hollow PG.

Elemental analysis

The EDX is a highly sensitive technique for the detection of various elements. EDX elemental analysis (Fig. 2) revealed that the HPGs were mostly composed of the carbon and oxygen atoms, which correspond to the sporopollenin structure that forms the exine shell.[30] The EDX pattern showed no peak for the nitrogen atom, verifying the absence of any nucleic acid/protein and therefore allergen-free nature of the prepared building blocks.

Protein and genetic material staining and imaging

Visible dye-based staining techniques were employed to further confirm the genetic materials and allergen proteins removal from PGs. For DNA detection, basic fuchsin (BF) was used according to the Feulgen technique. As shown in Fig. 3A, staining of raw PGs with BF resulted in the demonstration of DNA coloring and thus intensely colored generative nucleus, while staining of processed PGs (HPGs) revealed genetically-free shells (Fig. 3B). Coomassie brilliant blue (CBB) is a dye that binds to proteins with a high level of sensitivity and can be visualized by bioimaging. The resulted images of CBB staining demonstrated proteins extraction from the raw PGs forming the large inner cavities deprived of the allergenic proteins (Fig. 3C, D).

Cell-HPG building block interface

Surface reactivity is an essential factor influencing cell responses. The hAD-MSCs behavior at the interface with HPGs building blocks was indicated by FESEM. The obtained images demonstrated a bioactive cell-building

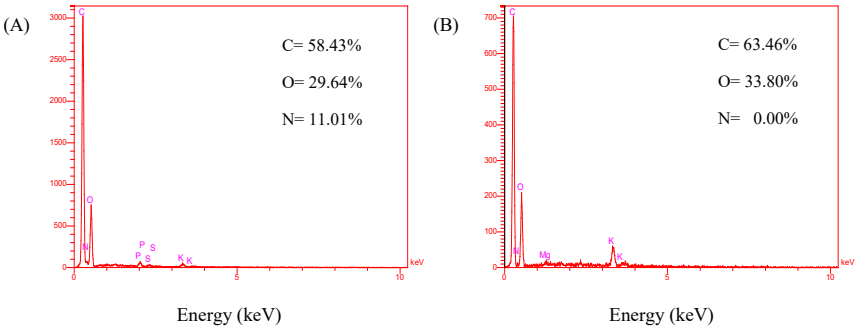

Fig. 2. EDX elemental analysis of *Pistacia vera* L. (A) Raw pollen grain (PG). (B) Hollow pollen grain (HPG).

block interface. Based on our findings (Fig. 4), the presence of HPGs was considered to provide better cell adhesion sites with excellent cellular biocompatibility, exhibiting normal cell morphology, attachment, and spreading.

Cytocompatibility

The metabolic activities of cultured hAD-MSCs on the HPGs building blocks were quantified using MTT assay (the absorbance of HPGs was subtracted from the resulted readings). The metabolic activities of cells were significantly ($P<0.05$) higher in the presence of HPGs compared to the scaffold-free condition during 21 days of culture (Fig. 5). Outstandingly, the reduced metabolic activity of hAD-MSCs after day 14 in the scaffold-free condition was improved by HPGs building blocks.

ALP activity

ALP colorimetric assay was carried out in growth medium condition (without osteogenic inducers) on days 7, 14, and 21 to study the effect of HPGs building blocks on the hAD-MSCs differentiation into osteoblast. The results showed that the level of ALP activity of the cells in the presence of HPGs was significantly ($P<0.05$) superior to the group cultured without scaffold in all days (especially on day 14) after cell culture (Fig. 6).

Expression of apoptotic genes

The biocompatibility of HPGs building blocks was examined by analysis of the mRNA expression of BAX, BCL2, and BAX/BCL2 ratio using qRT-PCR. As elucidated in Fig. 7, HPGs building blocks significantly ($P<0.05$)

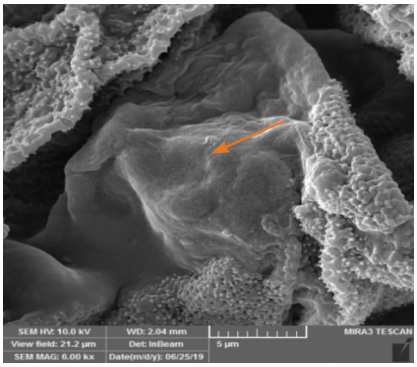

Fig. 4. FESEM image of hAD-MSCs cultured on the *Pistacia vera* L. HPGs building blocks on day 1. Arrow illustrates the cell adhered to the HPGs building block. HPG: hollow pollen grain.

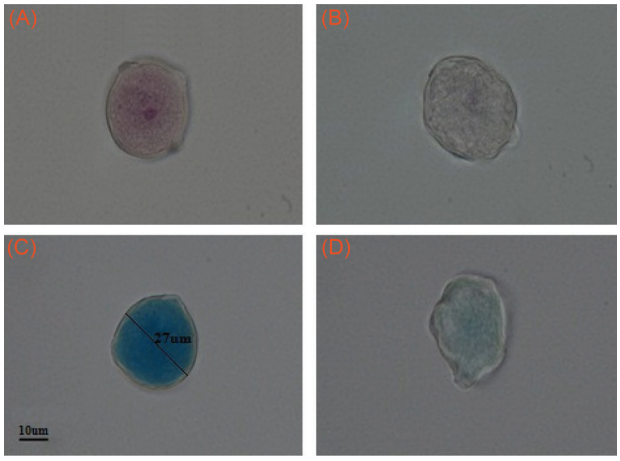

Fig. 3. Basic Fuchsin staining of genetic materials in *Pistacia vera L.* (A) Raw PG. (B) HPG. Coomassie Brilliant Blue staining of proteins in *Pistacia vera L.* (C) Raw PG. (D) HPG. Magnification: 100X. PG: pollen grain. HPG: hollow PG.

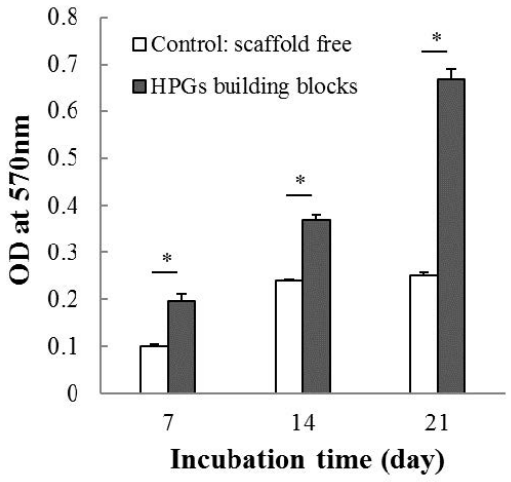

Fig. 5. Metabolic activities of hAD-MSCs on days 7, 14, and 21. The symbol (*) stands for a significant difference ($P<0.05$). HPG: hollow pollen grain.

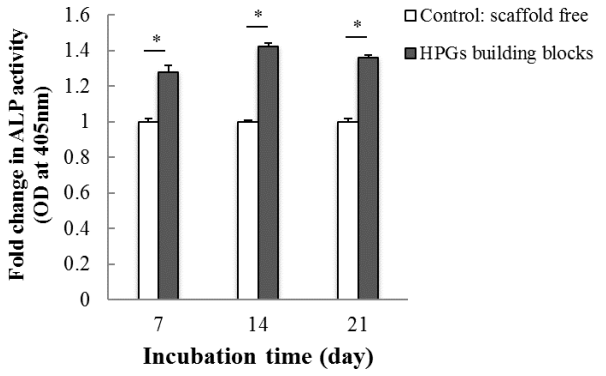

Fig. 6. Relative alkaline phosphatase activity of hAD-MSCs on the *Pistacia vera* L. HPGs building blocks on days 7, 14, and 21 as compared to the cells grown without scaffold. The symbol (*) stands for a significant difference (*P* value < 0.05). HPG: hollow pollen grain.

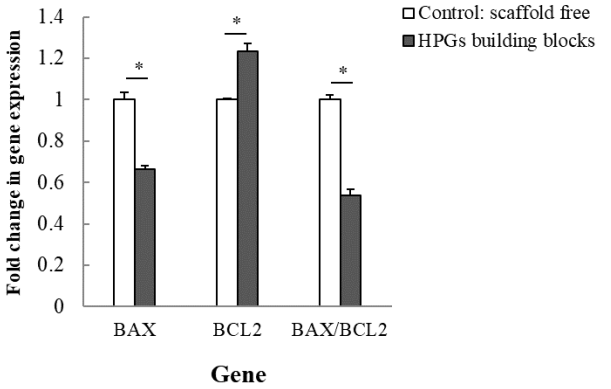

Fig. 7. The mRNA expression of *BAX*, *BCL2*, and *BAX*/*BCL2* ratio using the qRT-PCR analysis on day 21. *GAPDH* was used as a housekeeping gene. The symbol (*) stands for a significant difference (*P* value < 0.05). HPG: hollow pollen grain.

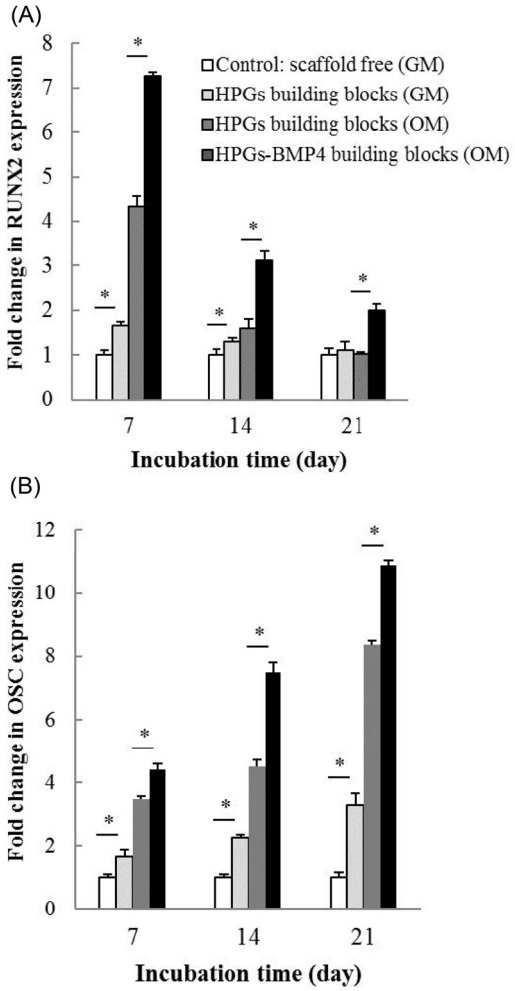

Fig. 8. The expressions of (A) *RUNX2* and (B) *OSC* genes analyzed using the qRT-PCR analysis on days 7, 14, and 21. *GAPDH* was used as a housekeeping gene. The symbol (*) stands for a significant difference (*P* value < 0.05). HPG: hollow pollen grain. GM: growth medium. OM: osteogenic medium.

decreased the expression level of BAX gene, while BCL2 expression was obviously increased. The expression ratio of BAX/BCL2 was found to be markedly declined in the cells interacted with HPGs.

Expression of osteogenic genes

Further, the osteoconductive potential of the HPGs building blocks was evaluated by the qRT-PCR analysis of the relevant genes. In this regard, the gene expression of *RUNX2* and *OSC* were evaluated as early and late bone development markers, respectively. To confirm the results of ALP test, cells were grown in the GM condition (Fig. 8). Compared to the control group, the hAD-MSCs cultured on HPGs building blocks exhibited a statistically higher level of *RUNX2* ($P < 0.05$) and OSC ($P < 0.05$) expression in all days of cell cultures, except for *RUNX2* that the rate of expression remained constant on day 21 between scaffold free and cells cultured on the HPGs building block. As presented in Fig. 8, the pattern of *RUNX2* expression showed a time-dependent reduction, reaching the lowest level ($P<0.05$) on day 21, whilst *OSC* was significantly elevated by day 21 ($P<0.05$) as compared to day 7 and 14. This is consistent with ascending bone development, and differentiation of MSCs toward osteoblasts.[31]

Additionally, the impact of BMP-4 encapsulation in HPGs was investigated using MSCs cultured in OM condition. Based on our findings (Fig. 8), cells cultured in OM condition showed significant upregulation of both genes ($P<0.05$), as compared to GM condition (with an exception of *RUNX2* level on day 21). Moreover, the data reveals that the highest increase of both genes ($P<0.05$) was observed in the cells that were cultured on HPGs-BMP4 building blocks.

Discussion

As the second transplanted tissue after blood, bone has been a topic of interest in TERM. The major challenge in TERM is to design ideal scaffolds for promoting tissue regeneration. The criteria of an ideal scaffold for bone remodeling include biocompatibility, biodegradability,

desired mechanical properties combined with flexibility to shape, suitable surface for the stable cell-scaffold interface, three-dimensional environment for bone growth, interconnected porous network, stimulatory effect on bone formation, and being commercially producible.[32] Such an ideal system can be achieved using multidisciplinary approaches combined with advanced materials. The current study demonstrated that nature-made micro PG of *P. vera* with unique compositional and surface decorative features provides the aforementioned features as an appropriate scaffolding building block. To engineer pollens as scaffolding devices with interior core and exterior shell usability, it is required to remove cytoplasm and surface coating components. In this regard, defatting pretreatment was used to remove pollen-coated lipids containing any possible surface allergens. To obtain intact HPGs, conventional alkaline and acidolysis methods were utilized with slight modifications. According to our results, acidolysis and high temperature during alkaline lysis had destructive effects on *P. vera* PGs. Instead, morphological and compositional analyses using FESEM-EDX, DNA, and protein staining techniques revealed that increasing the duration of KOH (5%) treatment from 12 to 24 hours when the temperature changed from 80°C to 25°C can result in the successful interior removal of the pollens, along with the maintenance of integrity and surface features at a nanoscale range. The final product was approximately achieved 21% of the PGs initial mass. The value of nitrogen in EDX analysis refers to the amount of the proteins and nucleic acids retained in the extracted pollen shells. Quantitative EDX analysis demonstrated a nitrogen-free and so protein/DNA-free construct of the prepared HPGs. Accordingly, as the proteins are mostly the main compounds to induce allergic reactions caused by pollens, this preparation strategy provides non-allergenic HPGs building blocks.[33,34] Further investigation using DNA and protein staining methods confirmed the complete elimination of genetic materials and proteins. The analysis by FESEM observation also confirmed the leakage of pollen cytoplasmic materials such as carbohydrates (e.g. starch granules) and protein bodies.

In the bottom-up tissue engineering approach, large complex 3D tissues are fabricated by assembling individual micro-engineered building blocks. One method in this approach is to pack surface-seeded micro-objects within the bioreactor. Such a system enables the formation of interconnected channels between the micro-object modules for vascularization and provides high access to cells for nutrients, gases, and metabolic wastes transportation.[35] Different plant species offer pollens in various shapes and surface ornamentations. The pollens from *P. vera* with suitable spherical bead-like shape microstructure provide a large surface-to-volume ratio, uniform cell seeding platform, as well as proper mass transfer. Furthermore, its round geometric structure reduces the flow-induced shear stress and harsh effect of collision in the circulating condition of bioreactors, preventing unspecific cellular differentiation.[36] Moreover, the unique surface decoration of *P. vera* PG may provide a great number of anchoring junctions. Therefore, in this preliminary *in-vitro* study, the performance of *P. vera* HPG microstructure was evaluated as a tissue engineering building block for bone generation, using hAD-MSCs. The biocompatibility of scaffolds is a necessary factor for biomedical applications. FESEM analysis revealed a bioactive interface between the cells and HPGs building blocks, as well as excellent biocompatibility. The hAD-MSCs exhibited suitable cell adhesion behavior on the designed building blocks. Stable focal adhesion plays a crucial role in cell functions and the development and maintenance of tissue. The measurement of cell viability is important in evaluating the scaffold capacity to support initial cell adhesion and subsequent cellular processes such as proliferation and differentiation. The results of the MTT assay indicated that the proliferative activity of hAD-MSCs seeded on HPGs building blocks has been steeply increased during 21 days of culture, while it seems to be stopped in the scaffold-free condition. As expected, using HPG as a scaffolding building block resulted in more cell adhesion, viability, and confluence, due to several factors, including a large ratio of surface to volume, surface functionality and homobrochate ornamentation, and strong antioxidant activities of the pollen exine attributed to the high level of phenolic compounds like flavonoids. Researches on surface engineering have shown that surface roughness and functional groups stimulate cell-adhesion interactions and provide a great number of anchorage points for proteins adsorption and subsequently, more cell adhesion, spreading, proliferation, as well as the production of ECM components.[37,38] Moreover, surface porosity may produce capillary forces for the promotion of cells attachment.[39]

The safety of HPGs building blocks for TERM applications using hAD-MSCs was also supported by qRT-PCR analysis of apoptosis-related gene expressions. The death or survival of a cell depends on the expression level of BAX/BCL2 ratio. BAX gene is an important regulator of the apoptosis process inducing cell death, while BCL2 suppresses BAX expression and inhibits the apoptosis.[40] Considering the significantly reduced gene expression of BAX/BCL2 ratio in cells seeded on the HPGs, it seems that developed building blocks maintain hAD-MSCs viability through preventing the mitochondrial apoptosis pathway. The antioxidant effect is the greatest defense mechanism against oxidative stress and apoptosis.[41] Accordingly, HPGs with strong antioxidants in the shells can inhibit the expression of apoptotic genes and cellular degeneration. Furthermore, the obtained result implicated the protective effect of HPGs on the hAD-MSCs and favors the potential application of HPGs in TERM.

In the osteogenesis process, the enzymatic activity of ALP is involved in the initial stages of bone

tissue formation and plays an essential role in ECM mineralization. ALP hydrolyzes phosphate esters into phosphates to form hydroxyapatite crystals for initiating mineral deposition in the ECM. Accordingly, the ALP activity was measured after 7, 14, and 21 days of culture to examine the osteoconductive ability of HPG building block. As an early marker, ALP activity displayed an increasing trend until day 14, followed by a decrease on day 21. The reduction of enzymatic activity after day 14 might be due to the later stages of differentiation. The result reflects the ECM maturation under the influence of HPGs building blocks.[42]

Furthermore, the osteoconductive potential of the introduced building blocks was evaluated by osteogenesis-related gene expression analysis. The mechanism of the MSCs transition into bone-forming osteoblastic cells is a well-orchestrated phenomenon of several relevant gene expressions, such as *RUNX2*, *ALP*, and *OSC*. Of these, *RUNX2* gene is a master switch of the ossification, which regulates the early osteogenesis. The *OSC* gene codes the bone-specific ECM protein and is commonly analyzed as a late marker of osteogenesis.[43] Based on our data, after 7 days of culture on HPGs building blocks, *RUNX2* gene expression was downregulated, while *OSC* exhibited an upregulated expression; such a pattern in the gene expression occurs during osteoblast maturation. In GM condition, compared to the scaffold-free group, higher expression of both genes was observed in the cell-seeded HPGs group, supporting the osteoconductive nature of *P. vera* HPG building block. Investigations have indicated that rough, porous, and functionalized surfaces, such as the surface of the prepared HPG building block, stimulate the osteoblast differentiation and bone mineralization process and support the formation of ECM components by providing a great number of anchoring junctions.[38,39]

An advanced scaffold system utilized in TERM applications should be able to encapsulate and release the bioactive factors crucial to tissue regeneration.[44] Different inducers of osteogenic differentiation, such as BMPs, are involved in the bone formation process. BMP4, as a member of the BMP family, belongs to the superfamily of the Transforming Growth Factor β (TGF β) and plays a critical role in the formation and retention of bone structure and function. BMP4 is a differentiation regulator that can individually trigger osteoblast phenotype and induce *RUNX2* expression.[45-47] It is noteworthy that, the large inner cavity of HPGs can provide a suitable microenvironment for loading bioactive compounds, such as growth factors and differentiation inducers, to direct cellular responses. According to our results obtained from gene expression analysis, the release of BMP4 from HPGs-BMP4 building blocks led to higher expression of osteogenesis-related genes (*RUNX2* and *OSC*) as compared to HPGs without BMP4 loading. Accordingly, the combination of BMP4 with osteoconductive property of HPG building block may have a synergistic effect on repairing bone defects.

Research Highlights

What is the current knowledge?

√ High temperature during treatment is a long-established part of the pollen interior removal procedure.

√ Currently, synthetic scaffolding building blocks have been used as cell supporting structures in bottom-up tissue engineering.

What is new here?

√ The common method used for pollen interior removal was improved to maintain the native form of the shell.

√ Suggesting pollen grains as dual-functional scaffolding building blocks with the simultaneous capability of cell culture and bioactive compounds loading.

Conclusion

This research lays the foundation for a new green therapeutic way of using nature-produced microstructures of *P. vera* PGs as scaffolding building blocks for modular tissue engineering. In this respect, the modified streamlined mild method was developed to produce intact nonallergic HPGs with the ability of encapsulation of bioactive compounds. The data demonstrated the destructive effects of acidolysis and high temperature during alkaline lysis on the PGs, which are long-established parts of the pollen interior removal procedures. The *in-vitro* investigation of hAD-MSCs responses on the *P. vera* HPGs building blocks indicated that strong antioxidant properties and natural nano-engineered functional surfaces of the HPGs can provide safe and the most bioactive surfaces for cells attachment, proliferation, and differentiation. Furthermore, incorporation of BMP4 into the HPGs building blocks had a synergistic effect on bone formation.

Acknowledgments

This article is a part of a Ph.D. thesis supported by the Drug Applied Research Center, Tabriz University of Medical Sciences. The authors would also like to thank the technical and financial support provided by the Research Center for Pharmaceutical Nanotechnology, Tabriz University of Medical Sciences.

Funding sources

This work was supported by the Drug Applied Research Center, Tabriz University of Medical Sciences (grant No. 58781).

Ethical statement

The authors declare that they have no ethical issues for humans and animals.

Competing interests

The authors declare that they have no known competing financial interests or personal relationships that could have appeared to influence the work reported in this paper.

Authors' contribution

SZ, KA, and YBK: Conceptualization; KA, JB, YO: Experiment design and study validation. YBK, AB, SZ: Experiment design, data handling,

and data analysis. The project was supervised by KA and JB. All the authors contributed to the writing and reviewing of the article.

References

1. Zhang K, Wang S, Zhou C, Cheng L, Gao X, Xie X, *et al.* Advanced smart biomaterials and constructs for hard tissue engineering and regeneration. *Bone Res* **2018**; 6: 31. https://doi.org/10.1038/s41413-018-0032-9
2. Perez RA, Seo S-J, Won J-E, Lee E-J, Jang J-H, Knowles JC, *et al.* Therapeutically relevant aspects in bone repair and regeneration. *Mate Today* **2015**; 18: 573-89. https://doi.org/10.1016/j.mattod.2015.06.011
3. Vo TN, Kasper FK, Mikos AG. Strategies for controlled delivery of growth factors and cells for bone regeneration. *Adv Drug Deliv Rev* **2012**; 64: 1292-309. https://doi.org/10.1016/j.addr.2012.01.016
4. Edalat F, Bae H, Manoucheri S, Cha JM, Khademhosseini A. Engineering approaches toward deconstructing and controlling the stem cell environment. *Ann Biomed Eng* **2012**; 40: 1301-15. https://doi.org/10.1007/s10439-011-0452-9
5. Chen M, Wang X, Ye Z, Zhang Y, Zhou Y, Tan WS. A modular approach to the engineering of a centimeter-sized bone tissue construct with human amniotic mesenchymal stem cells-laden microcarriers. *Biomaterials* **2011**; 32: 7532-42. https://doi.org/10.1016/j.biomaterials.2011.06.054
6. Leferink A, Schipper D, Arts E, Vrij E, Rivron N, Karperien M, *et al.* Engineered micro-objects as scaffolding elements in cellular building blocks for bottom-up tissue engineering approaches. *Adv Mater* **2014**; 26: 2592-9. https://doi.org/10.1002/adma.201304539
7. Urciuolo F, Imparato G, Totaro A, Netti PA. Building a tissue in vitro from the bottom up: implications in regenerative medicine. *Methodist Debakey Cardiovasc J* **2013**; 9: 213-7. https://doi.org/10.14797/mdcj-9-4-213
8. Barrier S, Mackenzie G, Atkin S. *Physical and Chemical Properties of Sporopollenin Exine Particles*: University of Hull; **2008**.
9. Qu Z, Meredith JC. The atypically high modulus of pollen exine. *J R Soc Interface* **2018**; 15: 20180533. https://doi.org/10.1098/rsif.2018.0533
10. Paunov VN, Mackenzie G, Stoyanov SD. Sporopollenin micro-reactors for in-situ preparation, encapsulation and targeted delivery of active components. *J Mater Chem* **2007**; 17: 609-12. https://doi.org/10.1039/B615865J
11. Rowley JR, Skvaria JJ, El-Ghazaly G. Transfer of material through the microspore exine - from the loculus into the cytoplasm. *Can J Bot* **2003**; 81: 1070-82. https://doi.org/10.1139/b03-095
12. Hamad SA, Dyab AFK, Stoyanov SD, Paunov VN. Encapsulation of living cells into sporopollenin microcapsules. *Journal of Materials Chemistry* **2011**; 21: 18018-23. https://doi.org/10.1039/C1JM13719K
13. Komosinska-Vassev K, Olczyk P, Kaźmierczak J, Mencner L. Bee pollen: chemical composition and therapeutic application. **2015**; 2015: 297425. https://doi.org/10.1155/2015/297425
14. Rzepecka-Stojko A, Stojko J, Kurek-Górecka A, Górecki M, Kabała-Dzik A, Kubina R, *et al.* Polyphenols from Bee Pollen: Structure, Absorption, Metabolism and Biological Activity. *Molecules* **2015**; 20: 21732-49. https://doi.org/10.3390/molecules201219800
15. Ylstra B, Touraev A, Moreno RM, Stöger E, van Tunen AJ, Vicente O, *et al.* Flavonols stimulate development, germination, and tube growth of tobacco pollen. *Plant Physiol* **1992**; 100: 902-7. https://doi.org/10.1104/pp.100.2.902
16. Wiermann R, Vieth K. Outer pollen wall, an important accumulation site for flavonoids. *Protoplasma* **1983**; 118: 230-3. https://doi.org/10.1007/BF01281807
17. Song Y, Ju Y, Song G, Morita Y. In vitro proliferation and osteogenic differentiation of mesenchymal stem cells on nanoporous alumina. *Int J Nanomedicine* **2013**; 8: 2745-56. https://doi.org/10.2147/ijn.s44885
18. Kieswetter K, Schwartz Z, Dean DD, Boyan BD. The role of implant surface characteristics in the healing of bone. *Crit Rev Oral Biol Med* **1996**; 7: 329-45. https://doi.org/10.1177/10454411960070040301
19. Ionescu LC, Mauck RL. Porosity and cell preseeding influence electrospun scaffold maturation and meniscus integration in vitro. *Tissue Eng Part A* **2013**; 19: 538-47. https://doi.org/10.1089/ten.TEA.2012.0052
20. Zhu Y, Liu T, Song K, Fan X, Ma X, Cui Z. Adipose-derived stem cell: a better stem cell than BMSC. *Cell Biochem Funct* **2008**; 26: 664-75. https://doi.org/10.1002/cbf.1488
21. Gimble JM, Katz AJ, Bunnell BA. Adipose-derived stem cells for regenerative medicine. *Circulation research* **2007**; 100: 1249-60.
22. Matousek P, Morris M. *Emerging Raman applications and techniques in biomedical and pharmaceutical fields*: Springer Science & Business Media; **2010**.
23. Schulte F, Lingott J, Panne U, Kneipp J. Chemical characterization and classification of pollen. *Anal Chem* **2008**; 80: 9551-6. https://doi.org/10.1021/ac801791a
24. Jensen WA. Botanical histochemistry. w. H. *HH Freeman and Company, San Francisco* **1962**.
25. Gahan PB. *Plant histochemistry and cytochemistry*: Academic Press; **1984**.
26. Quiroz FG, Posada OM, Gallego-Perez D, Higuita-Castro N, Sarassa C, Hansford DJ, *et al.* Housekeeping gene stability influences the quantification of osteogenic markers during stem cell differentiation to the osteogenic lineage. *Cytotechnology* **2010**; 62: 109-20. https://doi.org/10.1007/s10616-010-9265-1
27. Pfaffl MW, Horgan GW, Dempfle L. Relative expression software tool (REST) for group-wise comparison and statistical analysis of relative expression results in real-time PCR. *Nucleic Acids Res* **2002**; 30: e36. https://doi.org/10.1093/nar/30.9.e36
28. Edlund AF, Zheng Q, Lowe N, Kuseryk S, Ainsworth KL, Lyles RH, *et al.* Pollen from Arabidopsis thaliana and other Brassicaceae are functionally omniaperturate. *Am J Bot* **2016**; 103: 1006-19. https://doi.org/10.3732/ajb.1600031
29. Mert C. Pollen Morphology and Anatomy of Cornelian Cherry (Cornus mas L.) Cultivars. **2009**; 44: 519. https://doi.org/10.21273/hortsci.44.2.519
30. Mackenzie G, Boa AN, Diego-Taboada A, Atkin SL, Sathyapalan T. Sporopollenin, The Least Known Yet Toughest Natural Biopolymer. *Frontiers in Materials* **2015**; 2. https://doi.org/10.3389/fmats.2015.00066
31. Komori T. Regulation of osteoblast differentiation by Runx2. *Adv Exp Med Biol* **2010**; 658: 43-9. https://doi.org/10.1007/978-1-4419-1050-9_5
32. Martin RA, Yue S, Hanna JV, Lee PD, Newport RJ, Smith ME, *et al.* Characterizing the hierarchical structures of bioactive sol-gel silicate glass and hybrid scaffolds for bone regeneration. *Philos Trans A Math Phys Eng Sci* **2012**; 370: 1422-43. https://doi.org/10.1098/rsta.2011.0308
33. Diego-Taboada A, Maillet L, Banoub JH, Lorch M, Rigby AS, Boa AN, *et al.* Protein free microcapsules obtained from plant spores as a model for drug delivery: ibuprofen encapsulation, release and taste masking. *J Mater Chem B* **2013**; 1: 707-13. https://doi.org/10.1039/c2tb00228k
34. Diego-Taboada A, Barrier S, Thomasson M, Atkin S, Mackenzie G. Pollen: A novel encapsulation vehicle for drug delivery. *Innovations in Pharmaceutical Technology* **2007**; 63-8.
35. Leferink AM, Tibbe MP, Bossink E, de Heus LE, van Vossen H, van den Berg A, *et al.* Shape-defined solid micro-objects from poly(d,l-lactic acid) as cell-supportive counterparts in bottom-up tissue engineering. *Mater Today Bio* **2019**; 4: 100025. https://doi.org/10.1016/j.mtbio.2019.100025
36. Kim SH, Ahn K, Park JY. Responses of human adipose-derived stem cells to interstitial level of extremely low shear flows regarding differentiation, morphology, and proliferation. *Lab Chip* **2017**; 17: 2115-24. https://doi.org/10.1039/c7lc00371d
37. Neděla O, Slepička P, Švorčík V. Surface Modification of Polymer Substrates for Biomedical Applications. *Materials (Basel)* **2017**; 10. https://doi.org/10.3390/ma10101115
38. Boga JC, Miguel SP, de Melo-Diogo D, Mendonça AG, Louro RO,

Correia IJ. In vitro characterization of 3D printed scaffolds aimed at bone tissue regeneration. *Colloids Surf B Biointerfaces* **2018**; 165: 207-18. https://doi.org/10.1016/j.colsurfb.2018.02.038
39. Zhang K, Fan Y, Dunne N, Li X. Effect of microporosity on scaffolds for bone tissue engineering. *Regen Biomater* **2018**; 5: 115-24. https://doi.org/10.1093/rb/rby001
40. Kazemi N, Beigi Shahrestani S. Effect of Saffron Extract on Expression of Bax and Bcl-2 Genes in Gastric Adenocarcinoma Cell Line (AGS). *Gene Cell Tissue* **2018**; 5: e63608. https://doi.org/10.5812/gct.63608
41. Jalayeri M, Pirnia A, Najafabad EP, Varzi AM, Gholami M. Evaluation of alginate hydrogel cytotoxicity on three-dimensional culture of type A spermatogonial stem cells. *Int J Biol Macromol* **2017**; 95: 888-94. https://doi.org/10.1016/j.ijbiomac.2016.10.074
42. Jafary F, Hanachi P, Gorjipour K. Osteoblast Differentiation on Collagen Scaffold with Immobilized Alkaline Phosphatase. *Int J Organ Transplant Med* **2017**; 8: 195-202.
43. Han Y, Kim YM, Kim HS, Lee KY. Melatonin promotes osteoblast differentiation by regulating Osterix protein stability and expression. *Sci Rep* **2017**; 7: 5716. https://doi.org/10.1038/s41598-017-06304-x
44. De Witte TM, Fratila-Apachitei LE, Zadpoor AA, Peppas NA. Bone tissue engineering via growth factor delivery: from scaffolds to complex matrices. *Regen Biomater* **2018**; 5: 197-211. https://doi.org/10.1093/rb/rby013
45. Saskianti T, Yuliartanti W, Ernawati DS, Prahasanti C, Suardita K. BMP4 expression following stem cells from human exfoliated deciduous and carbonate apatite transplantation on rattus norvegicus. *Journal of Krishna Institute of Medical Sciences University* **2018**; 7: 56-61.
46. Scarfì S. Use of bone morphogenetic proteins in mesenchymal stem cell stimulation of cartilage and bone repair. *World J Stem Cells* **2016**; 8: 1-12. https://doi.org/10.4252/wjsc.v8.i1.1
47. Bruderer M, Richards RG, Alini M, Stoddart MJ. Role and regulation of RUNX2 in osteogenesis. *Eur Cell Mater* **2014**; 28: 269-86. https://doi.org/10.22203/ecm.v028a19